

Differences in cross-link chemistry between rigid and flexible dithiol-molecules revealed by optical studies of CdTe QDs

Supporting Information

R. Koole, B. Luigjes, R. Pool, T.J.H. Vlugt, M. Tachiya, C. de Mello Donegá, A. Meijerink, and D. Vanmaekelbergh

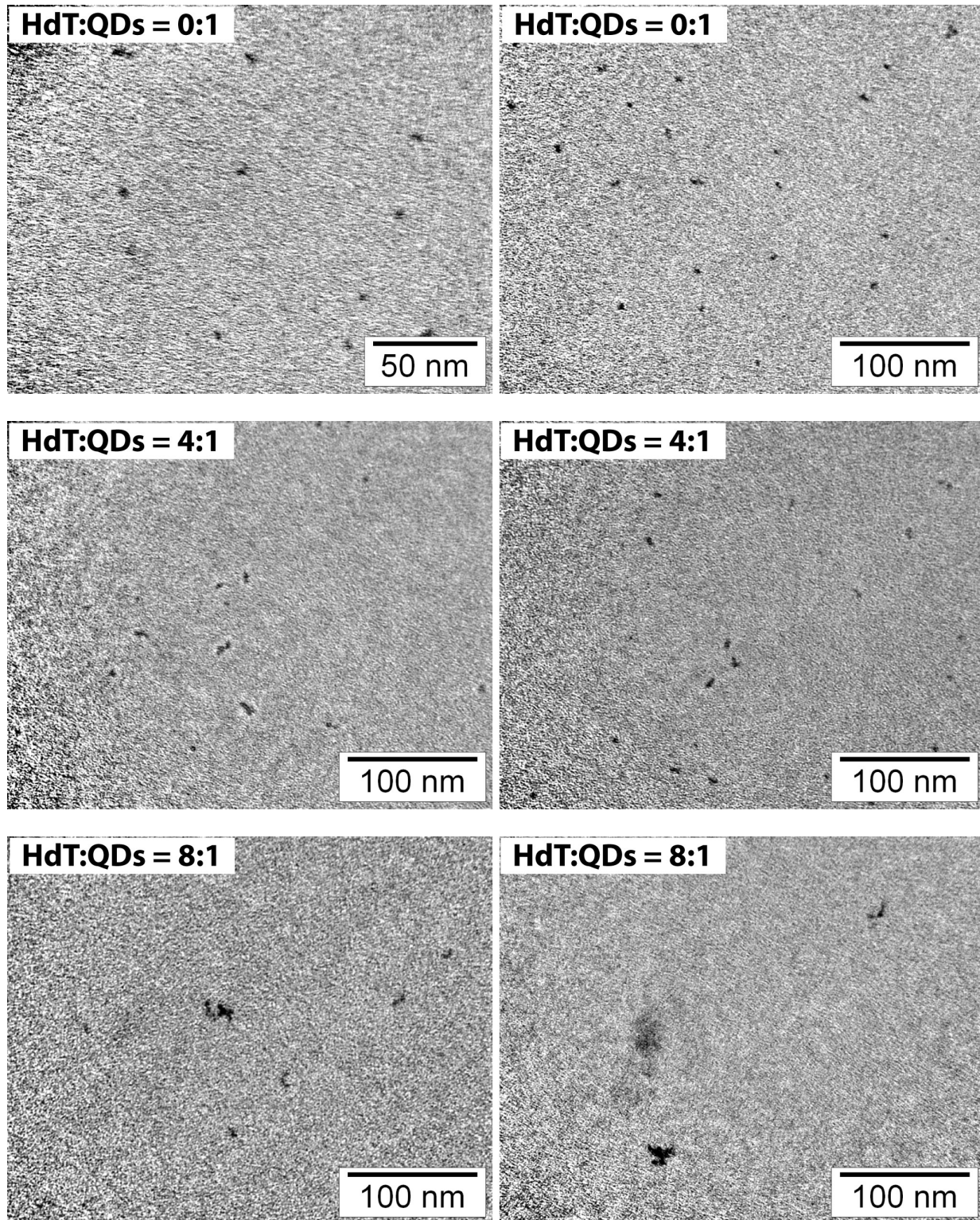
Debye Institute, Condensed Matter and Interfaces, Utrecht University, P.O. Box 80 000, 3508 TA Utrecht, The Netherlands

National Institute of Advanced Industrial Science and Technology, Tsukuba, Ibaraki 305-8565, Japan

Cryo-TEM images

Samples were prepared as follows: to 1 ml of the QD-dispersions that were used for the optical measurements, 1 ml of decaline was added. An aliquot of 3 μ l of this solution was pipetted onto an untreated Quantifoil 2/2 grid in the environmental chamber of a Vitrobot. The sample was blotted once during 0.5 s and rapidly plunged into liquid nitrogen. The grid was transferred to a Gatan cryoholder Model 626. The transmission electron microscope used was a Philips Tecnai12 equipped with a Biotwin-lens and a LaB6 filament. Images were captured with a SIS Megaview *II* CCD-camera and processed with AnalySIS software.

Figure S1 shows the result of cryo-TEM on the gQD-molecules at various linker/QD ratios using HdT as cross-linker molecule. Figure S2 shows the cryo-TEM images of gQD-molecules when BPD was used as cross-linker molecule.



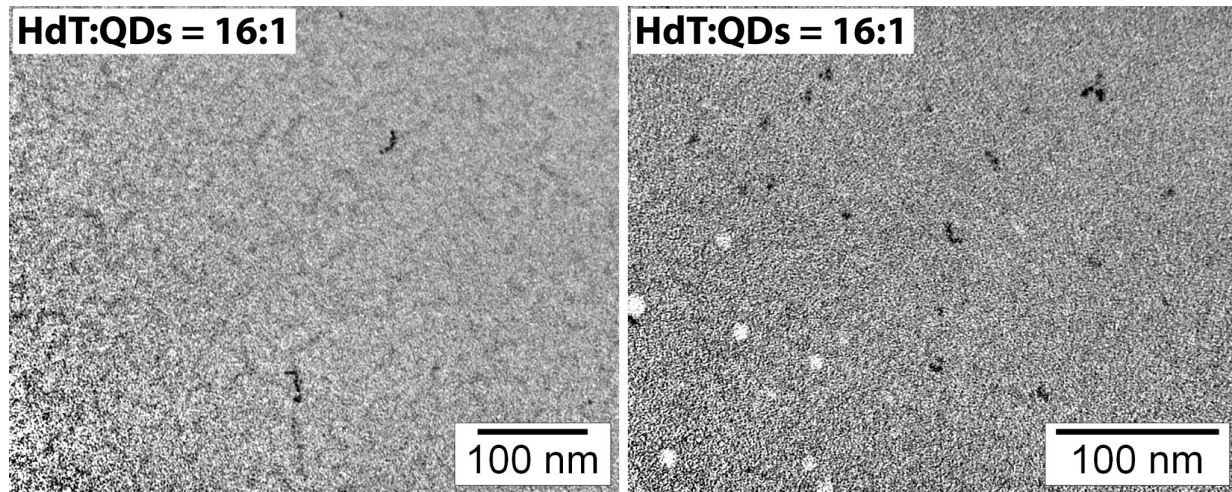
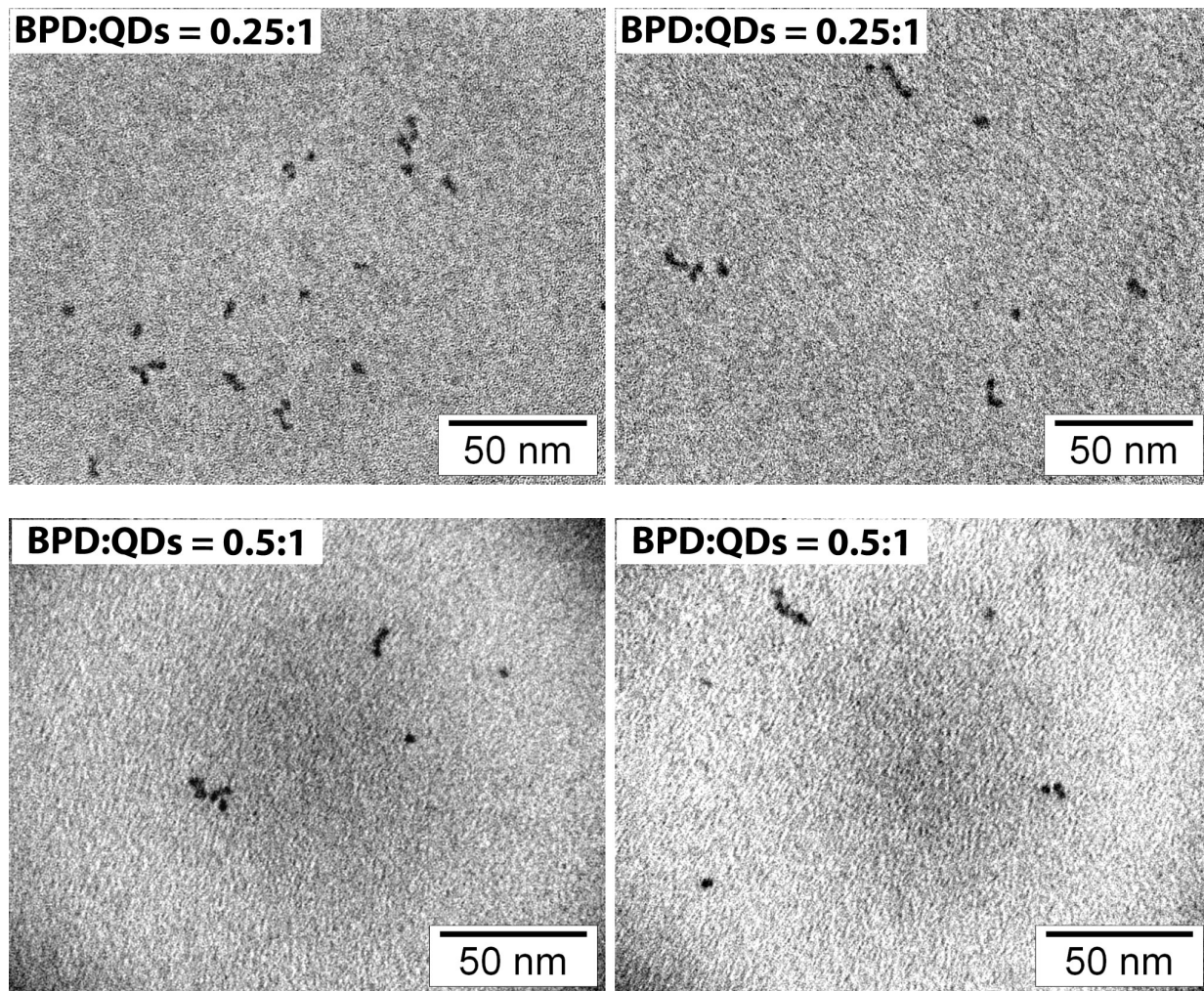


Figure S1 Cryo-TEM images of gQD-molecules at various linker/QD ratios, using HdT as the cross-linker molecule.



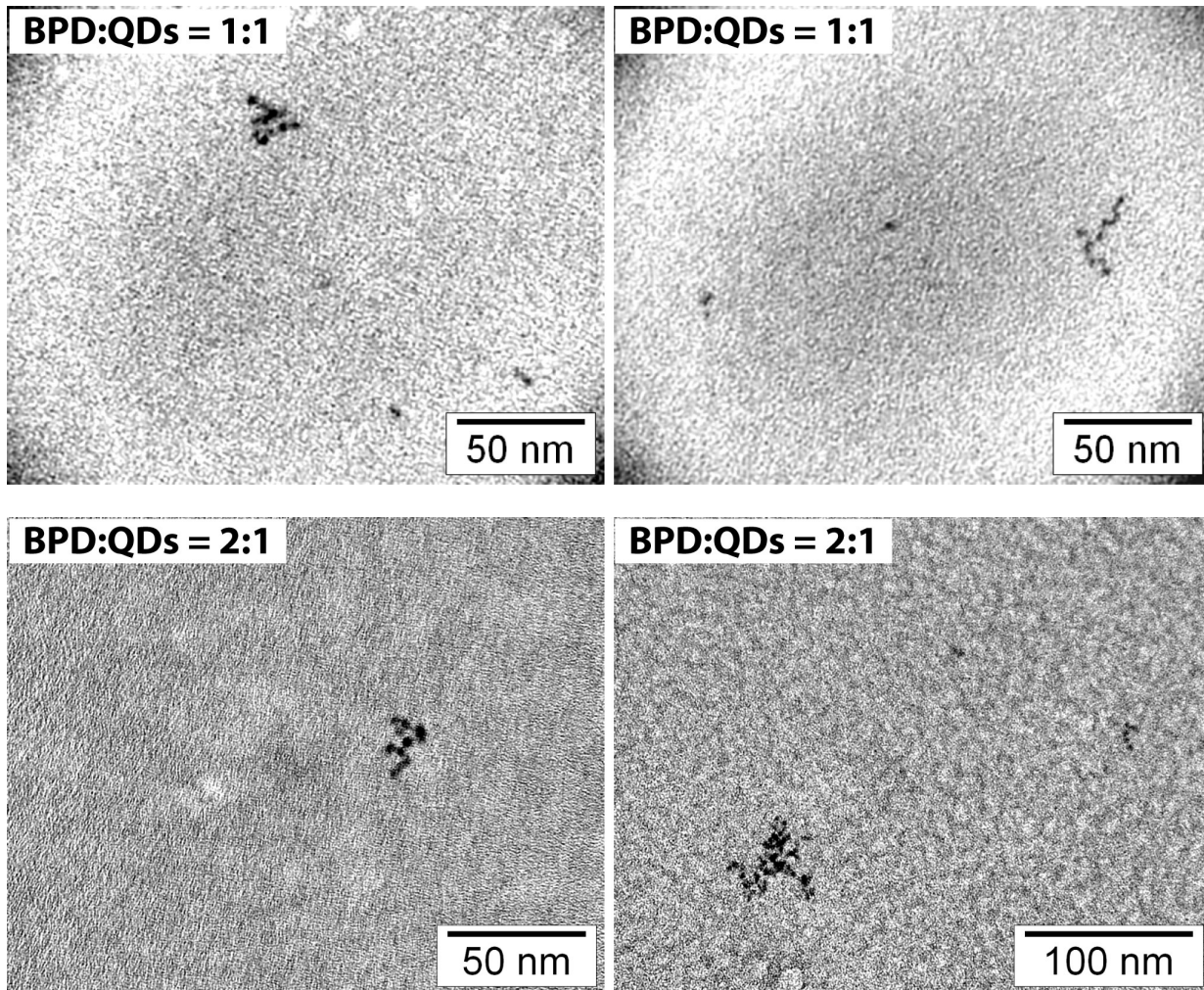


Figure S2 Cryo-TEM images of gQD-molecules at various linker/QD ratios, using BPD as the cross-linker molecule.

Molecular simulations

The snapshots shown in Figure 5 are taken from Monte Carlo (MC) simulations at constant NVT , where N is the total number of molecules, V is the volume of the simulation box and T the temperature. Both simulations were performed at $T = 300$ K in a cubic box with $V = 216$ nm 3 , applying periodic boundary conditions. The systems consisted of one rigid nanocrystal of 561 Au atoms (radius $R \approx 1$ nm), 6 hexane dithiol molecules, and 940 hexane (solvent) molecules. This composition corresponds to experimental conditions (e.g. temperature, atmospheric pressure). The solvent and dithiol molecules are represented by a united atom model where the contributions of the atoms in each functional group

(e.g. CH₂, CH₃ or SH) are incorporated in an effective pseudo atom. The intermolecular force field takes into account excluded volume and Van der Waals attraction. Within the chain molecules, we consider bond stretching, bond bending and torsional forces. The SH moieties interact stronger with the Au surface than other pseudo atoms. We performed two simulations: one where we used alkane-like torsional force constants for hexane dithiol (Figure 5a) and the other where we increased these constants for hexane dithiol by a factor of ten (Figure 5b). The latter should mimic rigid, aromatic dithiols. On average, one MC cycle consisted of

15 trial displacements, 15 trial rotations, 150 partial regrow trial moves and 750 full regrow trial moves. For both regrow moves we increased sampling efficiency by using the Configurational-bias Monte Carlo technique.^{S1} More information about the parameters used for the simulations can be found in a previous publication.^{S2}

Decay curves

It can be assumed in a good approximation that the number m of QDs attached to one QD follows a Poisson distribution given by

$$\varphi(m) = \left(\frac{n^m}{m!} \right) e^{(-n)} \quad (1)$$

where n is the average number of QDs attached to one QD. This assumes that the attachments of thiols to QDs are independent events that occur with a constant rate. When a QD is excited and has m QDs attached, the rate constant of the excited state decay for that QD is given by $\Gamma_{rad} + m\Gamma_{ET}$. Therefore, the ensemble averaged decay of the excited state is given by:

$$I(t) = I_0 \sum_m \varphi(m) e^{(-(\Gamma_{rad} + m\Gamma_{ET})t)} \quad (2)$$

It can be seen from equation (2) that the decay of the excited state is essentially described by multi-exponentials. Equation (2) can be re-written as follows, resulting in equation (3), which is used in the paper:

$$\begin{aligned}
 I(t) &= I_0 \sum_m \varphi(m) e^{-(\Gamma_{rad} + m\Gamma_{ET})t} \\
 &= I_0 \sum_m \left(\frac{n^m}{m!} \right) e^{(-n)} e^{-(\Gamma_{rad} + m\Gamma_{ET})t} \\
 &= I_0 e^{(-\Gamma_{rad}t - n)} \sum_m \frac{(n \cdot e^{(-\Gamma_{ET} \cdot t)})^m}{m!} \\
 &= I_0 e^{(-\Gamma_{rad}t - n)} \cdot e^{(n \cdot e^{(-\Gamma_{ET} \cdot t)})} \\
 &= I_0 e^{((- \Gamma_{rad}t) - n(1 - e^{(-\Gamma_{ET} \cdot t)}))} \tag{3}
 \end{aligned}$$

Not all decay curves that were fitted using equation (3) are shown in the paper. Figure S3a and S3b show the decay curves of green and red emitting CdTe QDs (black curves) cross-linked by HdT, and the corresponding fits (red solid lines). Figure S4 shows the decay curves and corresponding fits of gCdTe QDs cross-linked by BPD, at linker/QD ratios that were not shown in the paper.

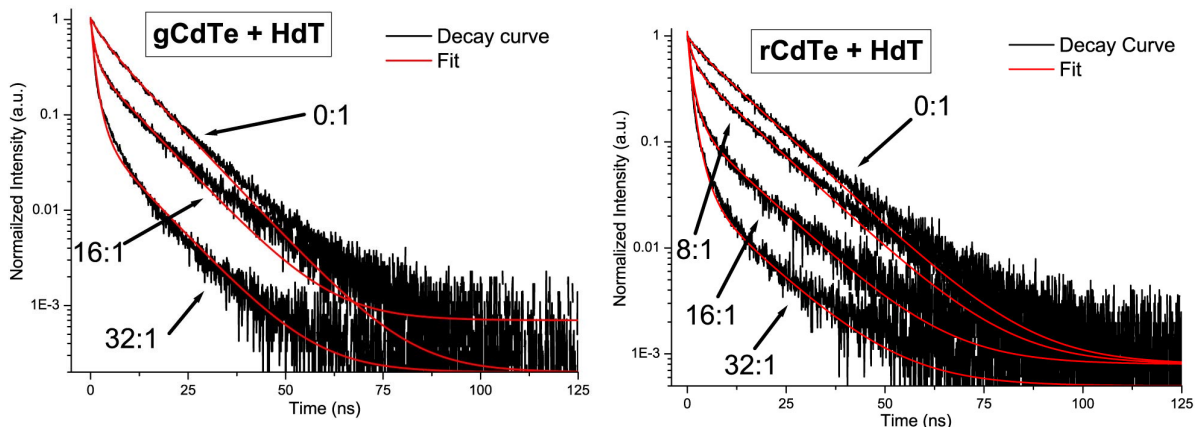


Figure S3 Decay curves and corresponding fits of (a) gCdTe and (b) rCdTe QDs at various HdT/QD ratios as indicated by the arrows. ($\lambda_{exc} = 406$ nm, $\lambda_{em} = 535$ nm (a) and 580 nm (b))

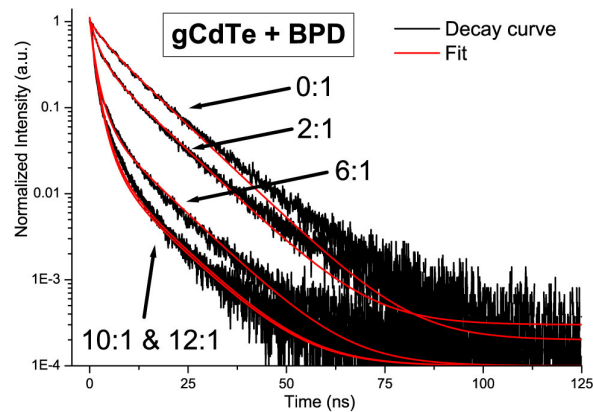


Figure S4 Decay curves and corresponding fits of gCdTe QDs at various BPD/QD ratios as indicated by the arrows. ($\lambda_{exc} = 406$ nm, $\lambda_{em} = 535$ nm)

- (S1) Frenkel, D.; Smit, B.; *Understanding Molecular Simulation* (Academic, New York, 2002), 2nd ed.
- (S2) Schapotschnikow, P.; Pool, R.; Vlugt, T.J.H. *Comput. Phys. Comm.* **2007**, accepted. doi: 10.1016/j.cpc.2007.02.028